Journal of Non-Crystalline Solids xxx (2010) xxx–xxx

Contents lists available at ScienceDirect

Journal of Non-Crystalline Solids

journal homepage: www.elsevier.com/ locate/ jnoncrysol

Optical absorption and structure of impurity Ni^{2+} center in tungstate–tellurite glass

V.G. Plotnichenko [a,*], V.O. Sokolov [a], G.E. Snopatin [b], M.F. Churbanov [b]

[a] Fiber Optics Research Center of the Russian Academy of Sciences 38 Vavilov Street, Moscow 119333, Russia
[b] Institute of Chemistry of High-Purity Substances of the Russian Academy of Sciences 49 Tropinin Street, Nizhny Novgorod 603600, Russia

ARTICLE INFO

Article history:
Received 11 February 2010
Available online xxxx

Keywords:
Tellurite glasses;
Defect centers;
Glasses containing transition metal ions;
Optical spectroscopy;
Computer simulation

ABSTRACT

Absorption spectra of Ni^{2+} ions in $22WO_3$–$78TeO_2$ tungstate–tellurite glass were studied and Ni^{2+} extinction coefficient spectral dependence was derived in the 450–2700 nm wavelength range. Computer modeling of the glass structure proved Ni^{2+} ions to be in trigonal-distorted octahedral environment in the tungstate–tellurite glass. Tanabe–Sugano diagram for such an environment was calculated and good description of the observed spectrum of Ni^{2+} ion was obtained. Basing on both absorption spectral range width and the extinction coefficient, nickel should be considered among the most strongly absorbing impurities in the tellurite glasses.

1. Introduction

Tellurite glasses are known to have wide transmission range (0.35–6.0 μm), high linear and nonlinear refractive indices and potentially low optical losses in the near- and mid-IR ranges. Because of this tellurite glasses are of considerable interest as materials for fiber optics applications. Glasses intended for optical fibers manufacturing should contain low amount of impurities responsible for optical loss. *3d* transition metals ions (V, Cr, Mn, Fe, Co, Ni and Cu) giving rise to intense absorption in the visible and near infrared region represent one of the main groups of the limiting impurities.

In the literature there are no quantitative data on the influence of 3*d* transition metal impurities on optical absorption in the transmission spectral range of tellurite glasses. On the other hand, absorption spectra of *3d* transition metal ions in zirconium fluoride- and silica-based glasses are studied to a considerable extent [1–5]. In zirconium fluoride-based glasses the optical absorption in the 1–2 μm range is limited by Co^{2+}, Fe^{2+} and Ni^{2+} impurities with extinction coefficient 100–500 dB km^{-1} ppm^{-1} [4]. Cr, Co, Fe and Cu impurities with extinction coefficient 300–700 dB km^{-1} ppm^{-1} in the silica transparency range, 1.3–1.6 μm, are known to be the most limiting impurities in silica fibers [5].

Extinction coefficient relates optical absorption intensity to impurities content. Hence knowledge of the extinction coefficient spectral dependence is needed, on the one hand, to control undesirable impurities content in optical materials using the materials' transmission spectra, to develop justified requirements for the acceptable content of impurities and to adjust technology to improve the optical parameters of materials; on the other hand, to control the content of dopants explicitly added to the material to optimize the characteristics of the developed lasers, optical amplifiers and converters.

The purpose of the present work is to study the transmission spectra of nickel-doped tungstate–tellurite glasses, WO_3–TeO_2 : Ni^{2+}, to determine the spectral dependence of Ni^{2+} extinction coefficient in the 450–2700 nm wavelength range and to relate absorption spectra of Ni^{2+} ions in the tungstate–tellurite glass with structure of their environment. Tungstate–tellurite glasses is known to be one of the most crystallization-resistant binary tellurite glasses. Nickel as a dopant is chosen for the investigation on account of its abundance in oxides used as raw materials and of the only valence state, +2, of nickel in oxides. The latter is of importance in view of oxidizing nature of TeO_2 as macro component of the glass under consideration.

2. Experimental

2.1. Preparation of Ni^{2+}-doped tungstate–tellurite glasses

Tungstate–tellurite glasses were prepared by cooling molten $22WO_3-78TeO_2$ high-purity oxides mixture [6]. TeO_2 and WO_3 oxides with nickel impurity content as low as $1.0 \cdot 10^{-4}$ wt.%Ni were used as raw components. Mixture of powdered raw components were pre-dried to remove water and then melted in platinum crucible heated by high-frequency inductor placed in oxygen atmosphere with 0.8 ppm humidity. The melt was homogenized for 1 h at a temperature of 800 °C (monitored by an optical pyrometer).

After homogenizing melting, part of the melt was solidified into $22WO_3-78TeO_2$ glass for later use to dilute nickel-doped glass melts. Nickel oxide was added to the rest of the melt to obtain doped glass

* Corresponding author. Tel.: +7 095 135 8093; fax: +7 095 135 8139.
E-mail address: victor@fo.gpi.ac.ru (V.G. Plotnichenko).

0022-3093/$ – see front matter © 2010 Elsevier B.V. All rights reserved.
doi:10.1016/j.jnoncrysol.2010.10.026

containing 1 wt.% NiO. Once the nickel-doped melt was homogenized, part of it was vitrified and the previously prepared $22WO_3-78TeO_2$ diluent glass was added to the rest of the melt in the crucible. Repeating the process several times, $22WO_3-78TeO_2 : Ni^{2+}$ glasses containing from 0.786 up to $9.4\cdot10^{-3}$ wt.% Ni were obtained. Nickel oxide concentration in the solidified glass was calculated from material balance equation.

$22WO_3-78TeO_2 : Ni^{2+}$ glasses samples with thickness from 0.5 to 50 mm with optically polished faces were prepared. Transmission spectra of these samples in visible and infrared spectral ranges were measured using Perkin Elmer Lambda 900 spectrophotometer (in the 400–3000 nm range) and Bruker IFS 113v Fourier spectrometer (in the 1000–10,000 nm range) with spectral resolution better than 4 nm.

2.2. Measurements

Fig. 1 shows transmission spectra of 0.5 mm-thick samples containing from 0.009 to 0.786 wt.% Ni. As viewed in Fig. 1, in the absorption spectrum of $22WO_3-78TeO_2 : Ni^{2+}$ glass there are two broad bands with maxima near 810 and 1320 nm and a band with maximum at wavelength <450 nm falling within the short-wavelength edge of $22WO_3-78TeO_2 : Ni^{2+}$ glass transparency range. The absorption intensity in all the bands increases with nickel content growth.

Transmission spectra were measured for the optical path length from 0.5 to 22 mm for samples with different nickel content. This allowed us to determine the extinction coefficient relating absorption of Ni^{2+} ion with concentration of such ions in $22WO_3-78TeO_2 : Ni^{2+}$ tellurite glass in the 450–2700 nm spectral range. By the way of example, Fig. 2 shows the light attenuation in the peak of the 1320 nm band in glasses containing 0.053 wt.% Ni vs. the sample thickness together with linear approximation of the experimental points. The *A* coefficient of the approximation is mostly due to Fresnel reflection losses and the line slope (*B* coefficient) represents the bulk absorption coefficient of the bulk glass with given nickel content.

In Fig. 3 are shown the experimental data and the approximation of the bulk absorption coefficient for the 1320 nm band for all the samples studied with Ni content up to approximately 0.12 wt.% Ni. As evident from Fig. 3, in this range of nickel content absorption in the maximum of the 1320 nm band is well fitted by a linear function of the absorbing Ni^{2+} ions concentration. The straight line slope

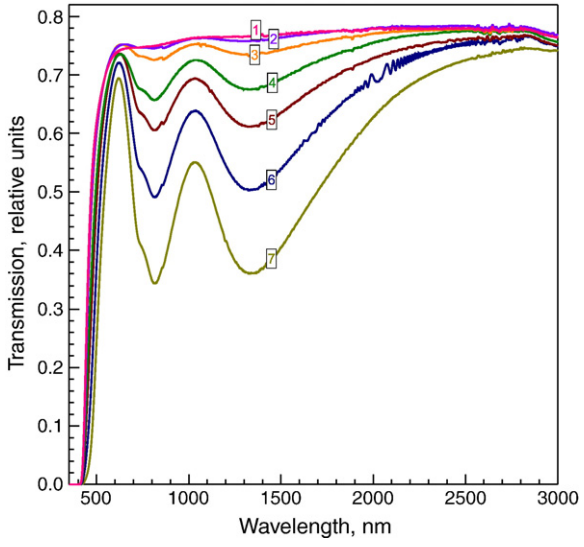

Fig. 1. Transmission spectra of $22WO_3–78TeO_2:Ni^{2+}$ tellurite glasses 0.5 mm-thick samples with different nickel oxide content (1 0.012, 2 0.029, 3 0.068, 4 0.16, 5 0.27, 6 0.51, and 7 1.01 wt.% NiO).

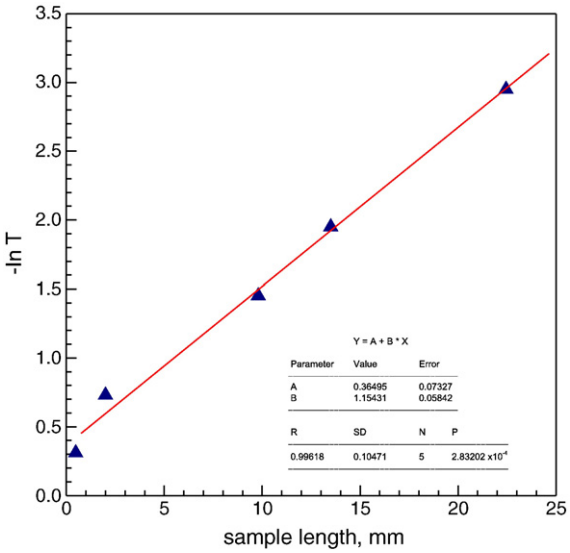

Fig. 2. Dependence of the radiation attenuation in the maximum of the 1320 nm absorption band in $22WO_3–78TeO_2:Ni^{2+}$ tellurite glasses containing 0.053 wt.% Ni on the sample length and its linear approximation.

representing the extinction coefficient is equal to 20.2 ± 0.8 cm^{-1} $(wt.\%\ Ni)^{-1}$ or 870 ± 35 $dB\,km^{-1}(wt.ppm\ Ni)^{-1}$.

Since both the number of absorption bands and their shapes do not depend on nickel content in the glass, it is possible to derive the spectral dependence of the extinction coefficient shown in Fig. 4. For reference, Table 1 presents Ni^{2+} impurity ions absorption at different wavelengths in several glasses with 1 ppm Ni content. The Ni^{2+} extinction coefficient spectral dependence allows us to estimate the content of impurity nickel ions in $22WO_3-78TeO_2 : Ni^{2+}$ tellurite glasses acceptable to get certain optical losses in glass at different wavelengths. Thus, optical losses as low as 100 dB km^{-1} in the 600–2000 nm spectral range are possible for nickel content not more than $1\cdot10^{-5}$ wt.% Ni or 0.1 wt. ppm Ni.

3. Modeling of the $WO_3–TeO_2:Ni^{2+}$ system

Modeling of the structure of impurity nickel centers in tungstate–tellurite glass network was performed using periodic model constructed on the basis of the supercell containing 32 TeO_2 groups (96

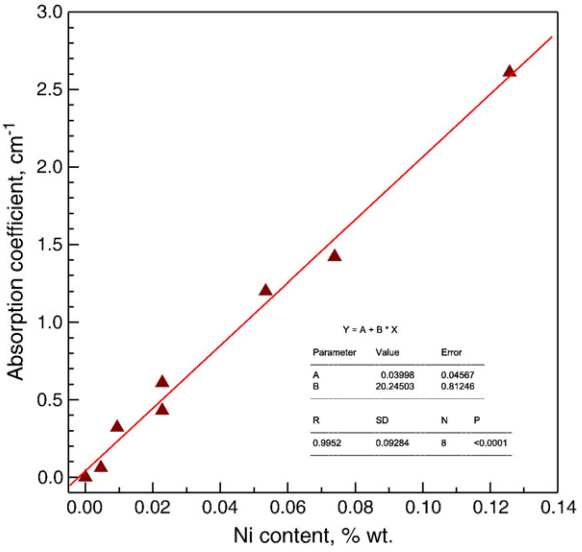

Fig. 3. Dependence of the bulk absorption coefficient at 1320 nm wavelength on the nickel content in $22WO_3–78TeO_2:Ni^{2+}$ tellurite glasses.

Please cite this article as: V.G. Plotnichenko, et al., Optical absorption and structure of impurity Ni^{2+} center in tungstate–tellurite glass, J. Non-Cryst. Solids (2010), doi:10.1016/j.jnoncrysol.2010.10.026

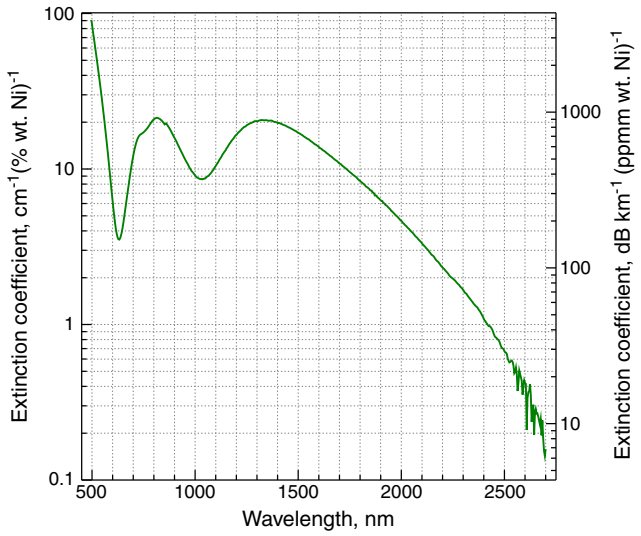

Fig. 4. Spectral dependence of the extinction coefficient of Ni^{2+} impurity ions in $22WO_3–78TeO_2:Ni^{2+}$ tellurite glass.

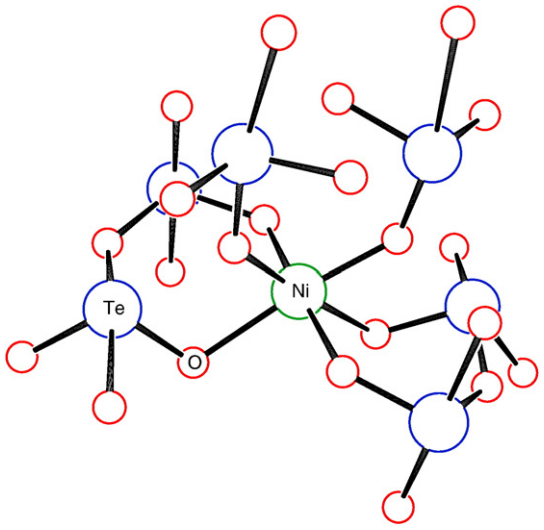

Fig. 5. Calculated configuration of Ni impurity atom in $WO_3–TeO_2$ tellurite glass network.

atoms in total), with the initial atoms arrangement corresponding to paratellurite lattice. Two TeO_2 groups in the supercell were substituted by NiO and WO_3 ones. So the supercell composition was $(NiO)(WO_3)(TeO_2)_{30}$. The described model was used to find the equilibrium configurations of impurity nickel atoms and tungsten atoms in the $WO_3—TeO_2$ tellurite glass network by means of ab initio (Car-Parrinello) molecular dynamics [7] with final complete geometry optimization by gradient method. All calculations were performed in the generalized gradient approximation of density functional theory in the plane waves basis using the Quantum-Espresso package [8]. Calculations were performed in two approaches, using either norm-conserving Troullier–Martins pseudopotentials [9] or ultrasoft pseudopotentials [10–12]. The norm-conserving Troullier–Martins pseudopotentials and ultrasoft pseudopotentials were developed for the tellurium, oxygen, nickel, and tungsten atoms with the help of fhi98PP [13] and USPP v. 7.3.6 [14] programs, respectively. *3d*, *4 s* and *4p* shells were taken to be the valence ones in the case of nickel atom.

Calculations showed that Ni^{2+} ion is sixfold coordinated in the $WO_3—TeO_2$ glass network ion, its environment being trigonally (D_3) distorted octahedron with oxygen atoms in its vertices forming Ni–O–Te linkages (Fig. 5). It should be remarked that Ni^{2+} turns out to be surrounded by pure TeO_2 network: no tungsten atom occurs in three nearest coordination shells.

Using the geometric parameters obtained in this modeling we calculated electronic states of Ni^{2+} ion in $WO_3—TeO_2$ glass network corresponding to d^8 electronic configuration of the Ni^{2+} ion. The calculation was performed using AOMX program [15] in angular overlap model of the ligand field theory [16–18]. The model parameters were optimized demanding the best reproduction of experimental values of the absorption bands wavelengths: the crystal field parameter $\Delta \approx 10988\,cm^{-1}$, Racah parameters $B \approx 958\,cm^{-1}$ ($\Delta/B \approx 11.5$) and $C \approx 3330\,cm^{-1}$, the angular overlap parameters $e_\sigma \approx 3663 cm^{-1}$ and $e_\pi \approx 183\,cm^{-1}$. With these parameters the Tanabe–Sugano diagram [19] was designed for Ni^{2+} in the d^8 electronic configuration in $WO_3—TeO_2$ glass network. The diagram is shown in Fig. 6 where the Δ/B parameter value corresponding to the Ni^{2+} absorption bands experimentally observed in $WO_3—TeO_2 : Ni^{2+}$ glasses and the transitions wavelengths are marked. Fig. 7 presents the scheme of calculated levels and main E1 transitions in octahedrally coordinated Ni^{2+} ion in the d^8 electronic configuration in $WO_3—TeO_2$ glass network both in O_h cubic and D_3 trigonal environments in comparison with free Ni^{2+} ion [20].

Results of the modeling allow us to interpret the observed absorption spectrum of Ni^{2+} ions in $WO_3—TeO_2 : Ni^{2+}$ glass as follows.

In the case of cubic O_h symmetry of the Ni^{2+} ion octahedral environment three main absorption bands are known to occur (see e.g. [21–23]). The bands correspond to spin-allowed E1 transitions from the ground state, $^3A_{2g}(^3F)$, to the excited states, $^3F_{2g}(^3F)$ ((a) transition in Fig. 7, typically in the 1100–1200 nm range); $^3F_{1g}(^3F)$

Table 1
Absorption (dB km^{-1}) caused by 1 wt. ppm impurity Ni^{2+} ions in various glasses.

Glass	Absorption band wavelength, μm				Ref.
	0.4	1.5	2.0	2.5	
ZrF_4-based (Zr–Ba–La–Al–Na–Pb–F)	650	200	90	30	[2]
ZrF_4-based (Zr–Ba–La–Al–Na–F)	360	100	<30	<3	[3]
SiO_2	2500	200	–	–	[5]
$22WO_3–78TeO_2$	>5000	750	200	30	This paper

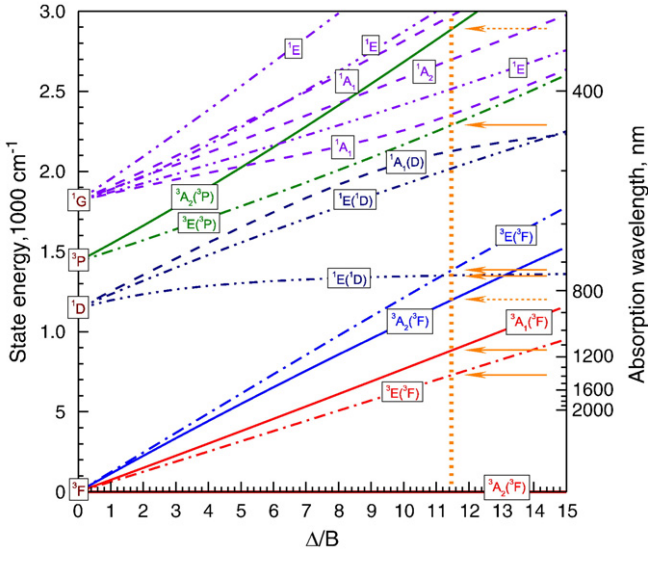

Fig. 6. Tanabe–Sugano diagram for Ni^{2+} ion in $WO_3–TeO_2:Ni^{2+}$ tellurite glass. Vertical dashed line corresponds to $\Delta/B \approx 11.5$. Wavelengths of D_3 symmetry-allowed and forbidden transitions are marked by solid and dashed arrows, respectively.

Please cite this article as: V.G. Plotnichenko, et al., Optical absorption and structure of impurity Ni^{2+} center in tungstate–tellurite glass, J. Non-Cryst. Solids (2010), doi:10.1016/j.jnoncrysol.2010.10.026

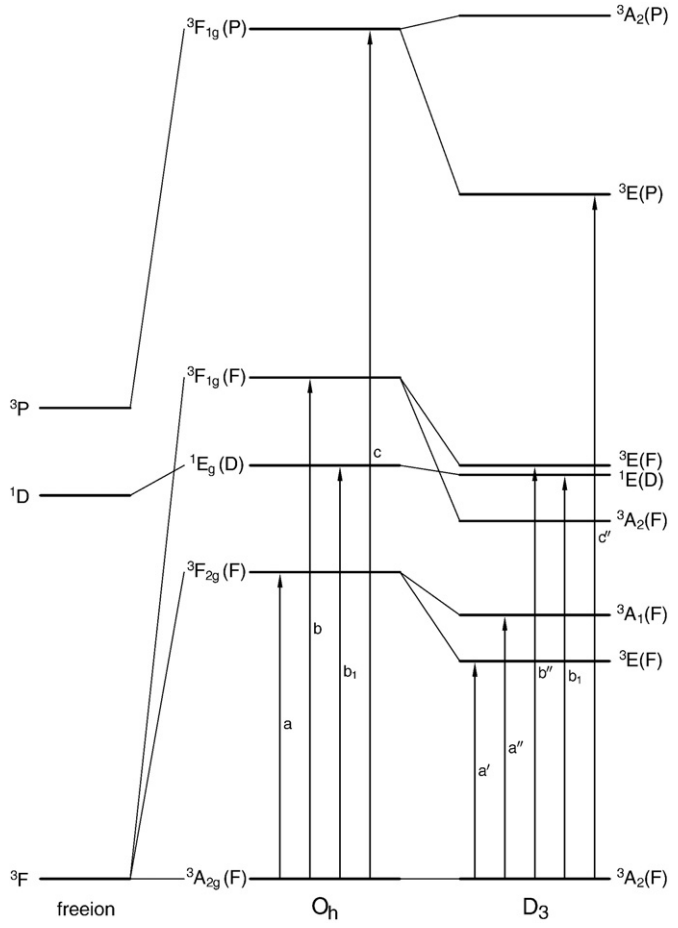

Fig. 7. Energy levels and main E1-transitions in octahedrally coordinated Ni^{2+} ion in the WO_3–TeO_2 glass network in d^8 electronic configuration in the cubic O_h and trigonal D_3 environment in comparison with free Ni^{2+} ion.

((b) transition in Fig. 7, typically in 630–770 nm range); and $^3F_{1g}(^3P)$ ((c) transition in Fig. 7, typically in 380–500 nm range).

Besides, weak absorption band caused by spin-forbidden transition from the $^3A_{2g}(^3F)$ ground state to the $^1E_g(^1D)$ excited state is sometimes observed near the (b) band ((b_1) transition in Fig. 7). Notice to avoid confusion that all these transitions are parity-forbidden but become slightly allowed owing to vibronic contributions. Calculation using the previously-listed parameters values yields the these transitions wavelengths for Ni^{2+} ion in O_h environment to be (a) 1000 nm, (b) 600 nm, (c) 350 nm, and (b_1) 723 nm, in satisfactory agreement with the typical values for O_h environment.

In D_{3d} or D_3 trigonally distorted octahedral environment of the Ni^{2+} ion, the ground state turns out to be $^3A_{2(g)}(^3F)$ and each of the $^3F_{1(g)}(^3F)$, $^3F_{2(g)}(^3F)$, and $^3F_{1(g)}(^3P)$ excited states is split into two states, $^3A_{1(g)}(^3F)$, $^3E_{(g)}(^3F)$; $^3A_{2(g)}(^3F)$, $^3E_{(g)}(^3F)$; $^3A_{2(g)}(^3P)$, $^3E_{(g)}(^3P)$, respectively. The $^1E_{(g)}(^1D)$ is not split. In the case of D_3 distortion E1 transitions from the $^3A_2(^3F)$ ground state to the excited $^3A_1(^3F)$, $^3E(^3F)$ and $^3E(^3P)$ turn out to be both spin- and symmetry-allowed ((a′), (a″), (b″) and (c″) transitions in Fig. 7) while transitions to the $^3A_2(^3F)$ and $^3A_2(^3P)$ excited states are symmetry-forbidden. In the case of D_{3d} distortion all the E1 transitions from the $^3A_{2g}(^3F)$ ground state to the $^3A_{1g}(^3F)$, $^3E_g(^3F)$, $^3E_g(^3P)$, $^3A_{2g}(^3F)$, and $^3A_{2g}(^3P)$ excited states, are symmetry-allowed. The transition from the $^3A_{2g}(^3F)$ ground state to the $^1E_g(^1D)$ excited one is still spin-forbidden ((b_1) transition in Fig. 7). The remark concerning the vibronic contributions remains valid.

In our case, (a′) and (a″) transitions from $^3A_{2(g)}(^3F)$ to $^3A_{1(g)}(^3F)$ and $^3E_{(g)}(^3F)$ correspond to the absorption band near 1300 nm; (b″) transition from $^3A_{2(g)}(^3F)$ to $^3E_{(g)}(^3F)$ corresponds to the absorption band near 800 nm; (b_1) transition from $^3A_{2(g)}(^3F)$ to $^1E_{(g)}(^1D)$ corresponds to the weakly pronounced band near 740 nm; and (c″) transition from $^3A_{2(g)}(^3F)$ to $^3E_g(^3P)$ corresponds to the absorption band in the <500 nm range.

Thus, in binary tungstate–tellurite glasses, due to strong trigonal distortion of the octahedral environment of Ni^{2+} ions, absorption bands of these ions turn out to be shifted substantially towards longer wavelengths in comparison with the absorption pattern typical for nickel-doped crystals. In this case, obviously, the IR absorption band (near 1320 nm) should be strongly heterogeneously broadened while the (heterogeneous) broadening of the other absorption bands should be relatively weak.

4. Summary

In this study we measured transmission spectra of $22WO_3-78TeO_2 : Ni^{2+}$ tungstate–tellurite glass samples containing from 1 to $1.2 \cdot 10^{-2}$ wt.% NiO and obtained spectral dependence of Ni^{2+} ions extinction coefficient in this glass in the 450–2700 nm wavelength range. These measurements together with our computer modeling of $WO_3-TeO_2 : Ni^{2+}$ glass structure suggest Ni^{2+} ions in such glasses to occur in strongly trigonally distorted octahedral sites. As a result, corresponding absorption bands are shifted significantly towards longer wavelengths compared to typical nickel-doped crystals and the absorption intensity being much higher than in silica- and zirconium fluoride-based glasses. So regarding both width of the absorption spectral range and the extinction coefficient value, nickel should be considered among strongly absorbing impurities in the tellurite glasses.

References

[1] G.R. Newns, P. Pantelis, D.L. Wilson, R.W.J. Uffen, R. Worthington, Opt. Quantum Electron. 5 (1973) 289.
[2] Y. Ohishi, S. Mitachi, T. Kanamori, T. Manabe, Phys. Chem. Glasses 24 (1983) 135.
[3] P.W. France, S.F. Carter, J.R. Williams, Mater. Sci. Forum 5 (1985) 353.
[4] C.R. Day, P.W. France, S.F. Carter, M.W. Moore, J.R. Williams Optical, Quantum Electron. 22 (1990) 259.
[5] P.C. Schultz, J. Am. Ceram. Soc. 57 (1974) 309.
[6] M.F. Churbanov, A.N. Moiseev, G.E. Snopatin, V.V. Dorofeev, V.G. Pimenov, A.V. Chilyasov, A.S. Lobanov, T.V. Kotereva, V.G. Plotnichenko, V.V. Koltashev, Yu.N. Pyrkov, Phys. Chem. Glasses 49 (2008) 297.
[7] R. Car, M. Parrinello, Phys. Rev. Lett. 55 (1985) 247.
[8] P. Giannozzi, S. Baroni, N. Bonini, M. Calandra, R. Car, C. Cavazzoni, D. Ceresoli, G.L. Chiarotti, M. Cococcioni, I. Dabo, A. Dal Corso, S. Fabris, G. Fratesi, S. de Gironcoli, R. Gebauer, U. Gerstmann, C. Gougoussis, A. Kokalj, M. Lazzeri, L. Martin-Samos, N. Marzari, F. Mauri, R. Mazzarello, S. Paolini, A. Pasquarello, L. Paulatto, C. Sbraccia, S. Scandolo, G. Sclauzero, A.P. Seitsonen, A. Smogunov, P. Umari, R.M. Wentzcovitch, J. Phys. Condens. Matter 21 (2009) 395502, (|http://www.quantum-espresso.org|).
[9] N. Troullier, J.L. Martins, Phys. Rev. B 43 (1991) 1993.
[10] D. Vanderbilt, Phys. Rev. B 41 (1990) 7892.
[11] K. Laasonen, R. Car, C. Lee, D. Vanderbilt, Phys. Rev. B 43 (1991) 6796.
[12] K. Laasonen, A. Pasquarello, C. Lee, R. Car, D. Vanderbilt, Phys. Rev. B 47 (1993) 10142.
[13] M. Fuchs, M. Scheffier, Comput. Phys. Commun. 119 (1999) 67.
[14] D. Vanderbilt, 2006, (|http://www.physics.rutgers.edu/dhv/uspp|).
[15] H. Adamsky, AOMX, an Angular Overlap Model Computer Program, Heinrich Heine Universitaet Duesseldorf, Theoretical Chemistry, 1995, (|http://www.aomx.de|).
[16] C.K. Jorgensen, J. Chem. Phys. 39 (1963) 1422.
[17] C.E. Schaeffier, Pure Appl. Chem. 24 (1970) 361.
[18] P.E. Hoggard, Optical Spectra and Chemical Bonding in Inorganic Compounds (Structure & Bonding vol.106). Springer, 2003, p. 37.
[19] Y. Tanabe, S. Sugano, J.Phys. Soc. Japan 9 (1954) 753; 9 (1954) 766.
[20] A.G. Shenstone, J. Opt. Soc. Am. 44 (1954) 749.
[21] L. Galoisy, G. Calas, Am. Mineral. 76 (1991) 1777.
[22] V.P. Solntsev, E.G. Tsvetkov, A.I. Alimpiev, R.I. Mashkovtsev, Phys. Chem. Miner. 33 (2006) 300.
[23] T. Suzuki, Y. Arai, Y. Ohishi, J. Lum. 128 (2008) 603.

Please cite this article as: V.G. Plotnichenko, et al., Optical absorption and structure of impurity Ni^{2+} center in tungstate–tellurite glass, J. Non-Cryst. Solids (2010), doi:10.1016/j.jnoncrysol.2010.10.026